DIVERSITY
SYNTIFIC Publisher
LOGIC JOURNAL MULTIDISCIPLINARY
E-ISSN 2988-571X
Vol. 2 Issue 3, 2024 Page.129-139

Original Article

FUNCTIONAL TESTING OF THE VARIABLE GEOMETRY SUSPENSION (VGS) PROTOTYPE ON BUMPY ROAD CONDITIONS

Dafa Aditya Murti[1)], Miftachul Huda[1)], Ferly Isnomo Abdi[1)], Diah Wulandari[1)], Firman Yasa Utama[1)]

[1)] Mechanical Engineering, Faculty of Vocational, State University of Surabaya, Indonesia
*Corresponding Author, E-mail: dafa.22070@mhs.unesa.ac.id

ABSTRACT

Background. Modern vehicles must prioritize comfort and safety, including the suspension system. While passive suspension systems are common, they struggle with excessive vibrations on uneven roads. Semi-active and active systems address this but are costly and complex. To solve this, a Variable Geometry Suspension (VGS) prototype was developed, integrating an active actuator into a passive system to adjust its geometry, providing performance comparable to active suspension systems.
Research Purpose. This study aims to examine the effect of single-link angle variations in the Variable Geometry Suspension (VGS) prototype on bumpy roads to determine the most comfortable single-link angle.
Research methods. This research employs a Research and Development (RnD) method by testing the single-link angle at 0°, 90° (reference angle), and 180°. Data collection was conducted by introducing road disturbances in the form of a bumpy road.
Findings. The testing results showed that the lowest Root Mean Square (RMS) value of the sprung-mass was at a single-link angle of 90°, with an RMS value of 0.72 m/s². This indicates a "Fairly Uncomfortable" level based on ISO 2631, with the damper on the unsprung-mass (c_t) and tire stiffness (k_t) disregarded, as well as the weight of the sprung-mass.
Conclusion. The VGS prototype's response to changes in the single-link angle on bumpy roads varies. However, the system effectively reduces vibrations at all angles, stabilizing the vehicle's body (sprung-mass) as the wheel (unsprung-mass) moves over uneven surfaces.

Keywords: Bumpy Road, Single-link Angle, Variable Geometry Suspension (VGS).

BACKGROUND

Transportation systems are experiencing rapid advancements, particularly in vehicles. People utilize vehicles to reduce travel time. In addition to shortening travel durations, vehicles must also prioritize driver safety and comfort. Comfort is achieved when a vehicle can effectively absorb vibrations caused by various road disturbances, while safety is ensured when the vehicle maintains sufficient traction between the tires and the road surface, minimizing the risk of slipping while driving [1]. Therefore, a suspension system is essential to address these needs.

The suspension system in vehicles is designed to support the load of the chassis and passengers while reducing vibrations caused by road disturbances [2]. Suspension control systems are categorized into passive, semi-active, and active suspension [3]. Passive suspension is a conventional system composed of springs and dampers without any control mechanism [4]. While it has a simple design and is easy to repair, passive suspension cannot dampen excessive vibrations under certain conditions, resulting in vibration emissions of 3 m/s², significantly reducing vehicle comfort [5]. This level of discomfort is classified as “very uncomfortable” according to the ISO 2631 standard [6]. Semi-active suspension,

which structurally resembles passive suspension, is designed to adapt its damping coefficient to reduce vibrations better [4]. Semi-active suspension achieves vibration emissions of 1.5 m/s², classified as "uncomfortable" by the ISO 2631 standard [5]. On the other hand, the active suspension uses active actuators installed in parallel with springs and dampers and utilizes sensor data to adjust damping, offering superior stability and comfort [3]. Active suspension is commonly used in luxury vehicles, which can reduce vibration emissions to 0.22 m/s² with Fractional Order Terminal Sliding Mode Controller, classified as "no vibration complaints" according to the ISO 2631 standard [7]. However, active suspension systems are expensive and have a complex design [3]. Research on Variable Geometry Suspension (VGS) has been conducted to address these limitations. VGS incorporates active actuator mechanisms, such as single-link and duo-link designs, into passive or semi-active suspension systems to control suspension geometry, thereby improving performance [8].

The testing of the VGS system was simulated using a full-car method through a quarter-car suspension system model. The results obtained will serve as a fundamental reference for the future design of vehicle suspension systems. Research simulated a complete vehicle travelling over a bumpy road while analyzing the performance of the front and rear wheels [9]. The study demonstrated improved comfort through a reduction in vertical acceleration by up to 62.4% and enhanced road holding by reducing vertical tire forces by 60.7% at the front and 54.8% at the rear. These findings provide insight into the comfort and safety performance of the VGS system compared to passive suspension systems, particularly when driving at high speeds on straight roads. However, the study of the VGS system using a quarter-car model remains limited to linear modelling, indicating the need for a more comprehensive approach to the actual design of the VGS system [10].

Based on this background, a Variable Geometry Suspension (VGS) prototype was designed to achieve optimal driving comfort using a quarter-car model with a double-wishbone suspension type. The modelling utilized road disturbances as bumpy roads, with a conveyor as the wheel driver. The input values for analyzing the performance of the VGS were obtained in the form of response graphs for each variation in the single-link angle. This study aims to examine the effect of single-link angle variations in the VGS prototype on bumpy roads to determine the most comfortable single-link angle.

RESEARCH METHOD

The research conducted is of the Research and Development (RnD) type, varying the single-link angles of 0°, 180°, and a reference single-link angle of 90° [10][11]. The VGS model is illustrated in Figure 1 and was subsequently redesigned, as shown in Figure 2, to enhance clarity. Finally, the design was implemented into a prototype, as depicted in Figure 3, for testing through a direct experimental approach.

This study utilizes bumpy road disturbances as input values for analysis. The bumpy road used has a height of 6 mm and a width of 45 mm, with a constant speed of 0.5 m/s (1.8 km/h). The purpose of the analysis is to evaluate the capability of the VGS system in reducing body vibrations across variations in the single-link angles of 0° and 180°, with a reference single-link angle of 90°, to determine the optimal angle for the VGS system during operation. Vibration measurements are conducted using an MPU 6050 accelerometer sensor on the quarter-car body (sprung-mass) and the vehicle wheel (unsprung-mass). The performance results are presented as acceleration graphs of the sprung-mass relative to the unsprung-mass. Additionally, each angle's Root Mean Square (RMS) values are analyzed to assess vibration emissions and compared against Table 1. RMS calculations are performed using the following formula [12]:

$$\sigma = \sqrt{\frac{1}{n}(\ddot{z}_{s_1}^{\ 2} + \ddot{z}_{s_2}^{\ 2} + \ddot{z}_{s_3}^{\ 2} + \cdots \ddot{z}_{s_n}^{\ 2})} \quad (1)$$

Where σ is the RMS value, $\ddot{z}_{s_1}^{\ 2};\ \ddot{z}_{s_2}^{\ 2}; \ldots \ddot{z}_{s_n}^{\ 2}$ are acceleration data points 1, 2, and so on, and n is the total number of data points.

Table 1. Comfort reactions to acceleration based on ISO 2631 [6]

Vibration Emission	Information
a < 0.315 m/s^2	Not uncomfortable
0.315 m/s^2 < a < 0.63 m/s^2	Comfortable
0.5 m/s^2 < a < 1 m/s^2	Fairly uncomfortable
0.8 m/s^2 < a < 1.6 m/s^2	Uncomfortable
1.25 m/s^2 < a < 2.5 m/s^2	Very uncomfortable
a > 2.5 m/s^2	Very uncomfortable

The parameters used are in Table 2. However, in this study, the damper on the unsprung-mass (c_t) and the tyre stiffness (k_t) are disregarded. Additionally, the weight of the sprung-mass of the VGS prototype needs to be addressed.

Table 2. VGS prototype parameters

Parameter	Symbol	value	Unit
Suspension spring deflection	δ	24	mm
Suspension spring solid length	L_S	8.8	mm
Suspension spring free length	L_F	36.4	mm
Suspension spring index	C	11.5	-
Suspension spring stiffness	k_s	0.58	N/mm
Dampers in suspension	c_s	1.8	Ns/mm
Conveyor torque	T	0.114	Nm
Conveyor power	P	4.18	watt

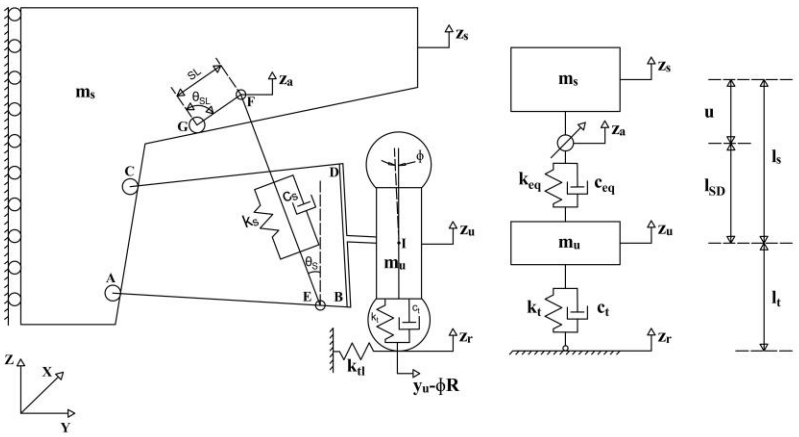

Figure 1. VGS modelling with double wishbone suspension [10]

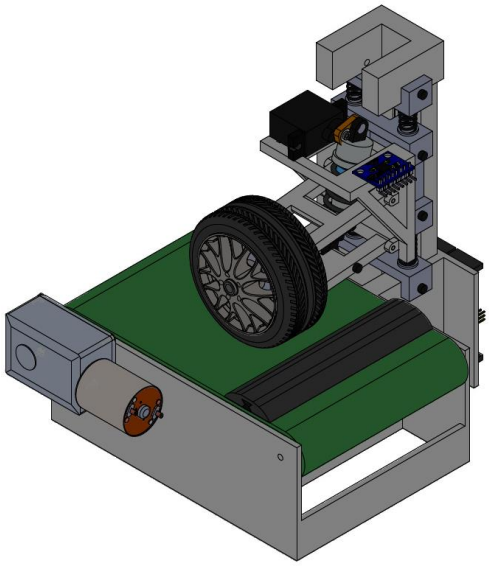

Figure 2. VGS prototype design

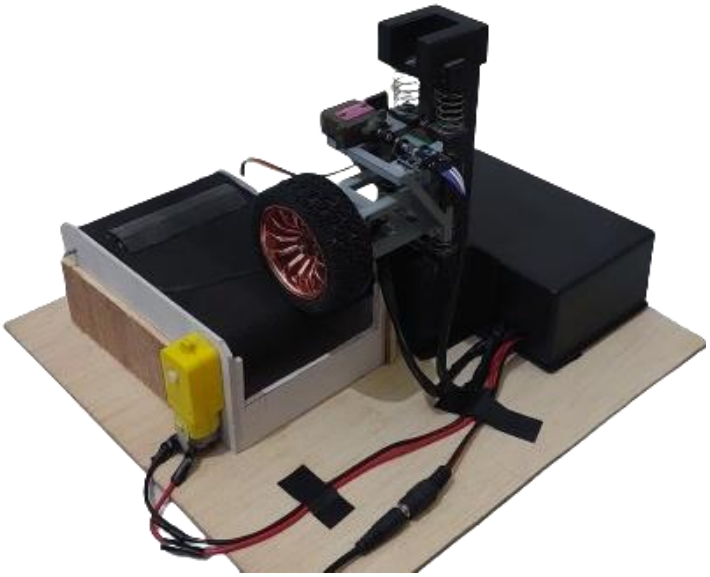

Figure 3. VGS prototype

FINDINGS

Acceleration Response at Single-Link Angles 0°, 90°, and 180° on a Bumpy Road

The tested VGS system uses a quarter-car model connected to a single-link controlled by a servo motor to adjust the angle, referred to as the VGS system. Additionally, a conveyor system is required to move the quarter-car wheel. The conveyor system generates a bumpy road input signal to analyze the VGS system's response. The response is measured using an accelerometer sensor (MPU 6050) placed near the wheel and on the vehicle body to compare vibrations between the body (sprung-mass) and the wheel (unsprung-mass) at different VGS angles. The experiment was conducted for 2 seconds with a measurement interval of 0.15 seconds. Data collection involved 3 trials, averaging the final results. The accelerometer sensor measurements at single-link angles of 0° (Table 3), 90° (Table 4), and 180° (Table 5) are presented.

Table 3. Acceleration Measurements at Single-Link Angle 0°

Time (s)	Experiment 1		Experiment 2		Experiment 3		Average	
	Acceleration (m/s^2)		Acceleration (m/s^2)		Acceleration (m/s^2)		Acceleration (m/s^2)	
	Sprung-mass	Unsprung-mass	Sprung-mass	Unsprung-mass	Sprung-mass	Unsprung-mass	Sprung-mass	Unsprung-mass
0	-0.4	-2.9	0.5	-1.9	1.1	0.4	0.4	-1.5
0.15	0.8	2.9	1.9	4.0	2.7	-3.8	1.8	1.0
0.3	0.5	6.1	0.8	3.4	-1.3	16.3	0.0	8.6
0.45	1.7	1.6	1.5	0.4	-0.7	1.6	0.8	1.2
0.6	-1.0	-4.8	0.6	7.5	2.2	-1.9	0.6	0.3
0.75	0.5	0.8	-0.1	-0.2	1.0	-1.1	0.5	-0.2
0.9	1.1	0.4	0.3	2.0	-0.1	-0.5	0.4	0.6
1.05	1.7	2.2	1.3	-1.3	-1.4	-0.4	0.5	0.2
1.2	0.5	-1.4	0.0	-0.9	0.3	-2.5	0.3	-1.6
1.35	0.9	1.4	-2.2	-4.9	-5.5	-14.8	-2.3	-6.1
1.5	0.4	1.0	0.1	-0.1	0.8	1.9	0.4	0.9
1.65	0.5	-0.6	1.1	0.1	1.7	4.8	1.1	1.4
1.8	0.3	0.5	-0.8	-0.7	-0.4	-0.8	-0.3	-0.3
1.95	-1.3	-0.3	0.3	2.4	0.7	-0.3	-0.1	0.6

Table 3. shows the acceleration vibrations of the sprung-mass and unsprung-mass caused by a bumpy road, measured using an accelerometer sensor. The highest average acceleration of the sprung-mass is 2.3 m/s², while the unsprung-mass exhibits higher vibrations with an average acceleration of 8.6 m/s². The response comparison of sprung-mass and unsprung-mass acceleration at a single-link angle of 0° can be seen in the graph in Figure 4.

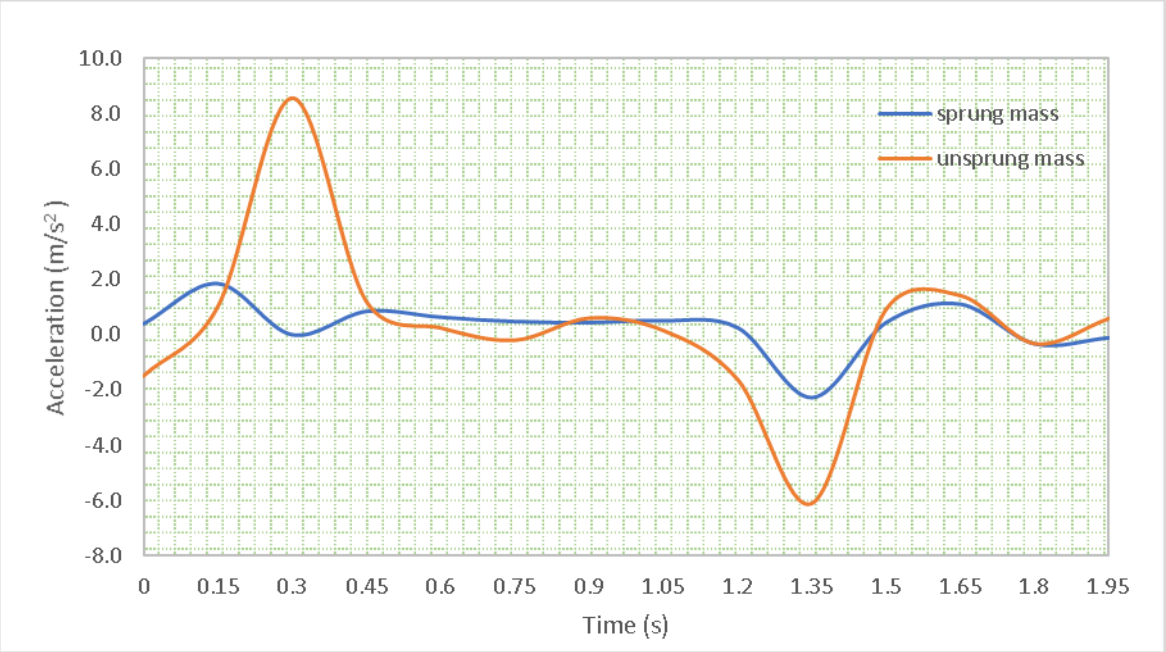

Figure 4. Acceleration response of the sprung-mass and unsprung-mass at a single-link angle of 0°.

Table 4. Acceleration Measurements at Single-Link Angle 90°

Time (s)	Experiment 1		Experiment 2		Experiment 3		Average	
	Acceleration (m/s^2)		Acceleration (m/s^2)		Acceleration (m/s^2)		Acceleration (m/s^2)	
	Sprung-mass	Unsprung-mass	Sprung-mass	Unsprung-mass	Sprung-mass	Unsprung-mass	Sprung-mass	Unsprung-mass
0	0.5	0.1	0.2	-3.2	0.5	0.7	0.4	-0.8
0.15	-0.4	4.8	1.3	-4.6	0.1	-7.1	0.3	-2.3
0.3	1.0	2.0	1.8	15.8	1.4	15.8	1.4	11.2
0.45	-3.6	15.8	0.8	3.6	3.8	-4.2	0.3	5.1
0.6	-0.6	3.5	0.7	-5.9	-0.3	-5.4	-0.1	-2.6
0.75	-0.3	-2.4	-1.4	0.4	-1.2	-5.2	-1.0	-2.4
0.9	0.6	0.9	-0.6	2.2	-1.0	-4.2	-0.3	-0.4
1.05	0.7	2.1	-0.6	0.3	-0.3	-3.8	0.0	-0.4
1.2	-0.7	0.0	-0.5	10.5	1.2	-1.1	0.0	3.2
1.35	-2.8	-13.2	-3.8	-19.8	2.5	-18.3	-1.4	-17.1
1.5	2.0	-1.2	-0.4	0.2	2.0	-0.5	1.2	-0.5
1.65	-0.8	-2.3	0.1	-0.7	-1.2	2.1	-0.6	-0.3
1.8	1.0	3.8	-0.4	-1.3	-0.6	-1.8	0.0	0.2
1.95	0.4	3.1	0.8	1.8	-1.2	-2.1	0.0	0.9

Table 4. shows the acceleration vibrations of the sprung-mass and unsprung-mass caused by a bumpy road, measured using an accelerometer sensor. The highest average acceleration of the sprung-mass is 1.4 m/s², while the unsprung-mass exhibits higher vibrations with an average acceleration of 17.1 m/s². The response comparison of sprung-mass and unsprung-mass acceleration at a single-link angle of 90° can be seen in the graph in Figure 5.

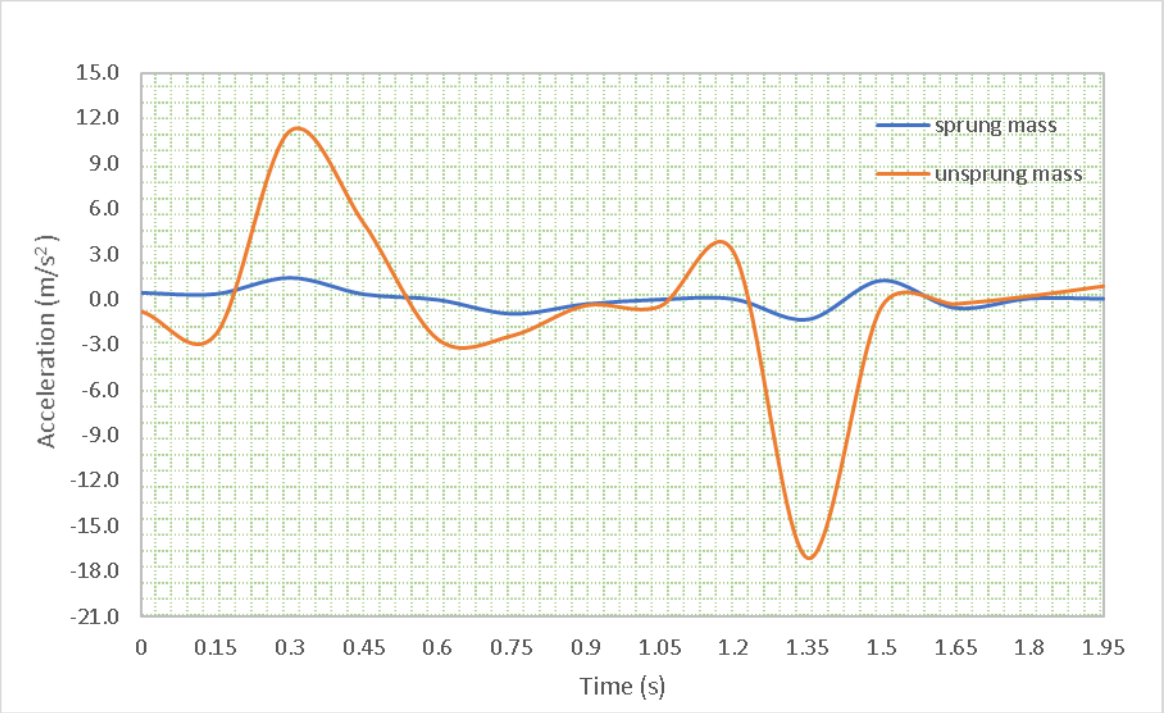

Figure 5. Acceleration response of the sprung-mass and unsprung-mass at a single-link angle of 90°.

Table 5. Acceleration Measurements at Single-Link Angle 180°

Time (s)	Experiment 1		Experiment 2		Experiment 3		Average	
	Acceleration (m/s^2)		Acceleration (m/s^2)		Acceleration (m/s^2)		Acceleration (m/s^2)	
	Sprung-mass	Unsprung-mass	Sprung-mass	Unsprung-mass	Sprung-mass	Unsprung-mass	Sprung-mass	Unsprung-mass
0	-0.3	0.7	1.5	-2.6	-1.1	-4.1	0.0	-2.0
0.15	0.8	1.3	4.1	16.3	4.4	16.3	3.1	11.3
0.3	0.7	2.6	-1.8	-7.5	-1.0	-3.7	-0.7	-2.9
0.45	1.4	12.8	-0.2	-8.7	0.4	0.6	0.5	1.6
0.6	-0.2	-6.5	0.5	-4.4	1.4	-0.6	0.6	-3.8
0.75	-0.2	0.6	0.2	5.0	0.6	-2.9	0.2	0.9
0.9	0.5	1.6	-0.4	1.5	0.2	3.5	0.1	2.2
1.05	0.5	1.3	0.0	-2.1	1.0	-2.9	0.5	-1.3
1.2	-0.4	0.1	0.3	-3.6	7.4	-25.4	2.4	-9.6
1.35	-0.7	1.8	1.1	4.3	-2.3	-3.8	-0.6	0.7
1.5	1.1	-1.6	0.7	1.1	-0.1	1.7	0.6	0.4
1.65	1.7	4.0	1.0	0.7	0.5	-1.0	1.1	1.2
1.8	1.0	2.3	0.7	-1.8	0.4	1.0	0.7	0.5
1.95	-0.2	-2.9	0.2	0.7	0.2	3.8	0.1	0.5

Table 5. shows the acceleration vibrations of the sprung-mass and unsprung-mass caused by a bumpy road, measured using an accelerometer sensor. The highest average acceleration of the sprung-mass is 3.1 m/s², while the unsprung-mass exhibits higher vibrations with an average acceleration of 11.3 m/s². The response comparison of sprung-mass and unsprung-mass acceleration at a single-link angle of 180° can be seen in the graph in Figure 6.

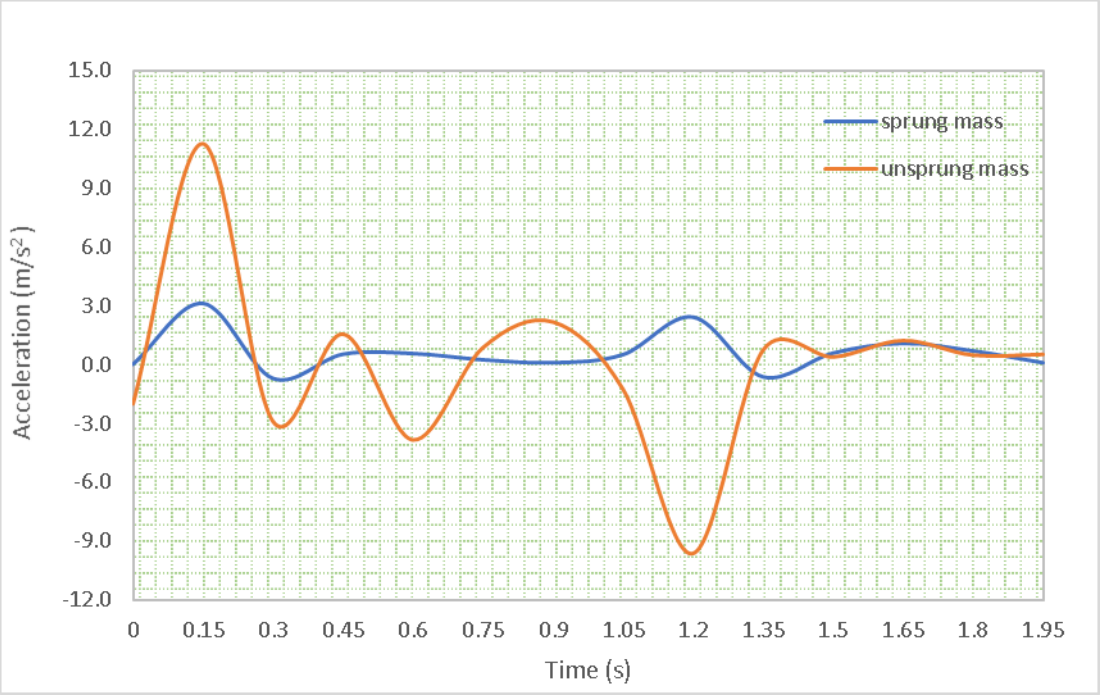

Figure 6. Acceleration response of the sprung-mass and unsprung-mass at a single-link angle of 180°.

The collected data is then used to calculate the Root Mean Square (RMS) value to evaluate the comfort level of the tested VGS system at each single-link angle based on ISO 2631 [6]. Therefore, the RMS value can be calculated as follows:

1. Sprung-mass acceleration at a single-link angle of 0°.

$$\sigma = \sqrt{\frac{1}{n}(\ddot{z}_{s_1}^{\,2} + \ddot{z}_{s_2}^{\,2} + \ddot{z}_{s_3}^{\,2} + \cdots \ddot{z}_{s_n}^{\,2})}$$

$$\sigma = \sqrt{\frac{1}{14}(0{,}4^2 + 1{,}8^2 + 0{,}0^2 + 0{,}8^2 + 0{,}6^2 + 0{,}5^2 + 0{,}4^2 + 0{,}5^2 + 0{,}3^2 + 2{,}3^2 + 0{,}4^2 + 1{,}1^2 + 0{,}3^2 + 0{,}1^2)}$$

$$\sigma = 0{,}92\ m/s^2$$

2. Sprung-mass acceleration at a single-link angle of 90°.

$$\sigma = \sqrt{\frac{1}{n}(\ddot{z}_{s_1}^{\,2} + \ddot{z}_{s_2}^{\,2} + \ddot{z}_{s_3}^{\,2} + \cdots \ddot{z}_{s_n}^{\,2})}$$

$$\sigma = \sqrt{\frac{1}{14}(0{,}4^2 + 0{,}3^2 + 1{,}4^2 + 0{,}3^2 + 0{,}1^2 + 1{,}0^2 + 0{,}3^2 + 0{,}0^2 + 0{,}0^2 + 1{,}4^2 + 1{,}2^2 + 0{,}6^2 + 0{,}0^2 + 0{,}0^2)}$$

$$\sigma = 0{,}72\ m/s^2$$

3. Sprung-mass acceleration at a single-link angle of 180°.

$$\sigma = \sqrt{\frac{1}{n}(\ddot{z}_{s_1}^{\,2} + \ddot{z}_{s_2}^{\,2} + \ddot{z}_{s_3}^{\,2} + \cdots \ddot{z}_{s_n}^{\,2})}$$

$$\sigma = \sqrt{\frac{1}{14}(0{,}0^2 + 3{,}1^2 + 0{,}7^2 + 0{,}5^2 + 0{,}6^2 + 0{,}2^2 + 0{,}1^2 + 0{,}5^2 + 2{,}4^2 + 0{,}6^2 + 0{,}6^2 + 1{,}1^2 + 0{,}7^2 + 0{,}1^2)}$$

$\sigma = 1{,}2\ m/s^2$

Based on these calculations, the RMS values for each single-link angle can be categorized for comfort according to ISO 2631, as shown in Table 6.

Table 6. Average RMS Values for Each Single-Link Angle

Single-link Angle	RMS Value (m/s^2)	According to ISO 2631	Range Vibration Emision
0^o	0.92	*Uncomfortable*	$0.8\ m/s^2 < a < 1.6\ m/s^2$
90^o	0.72	*Fairly uncomfortable*	$0.5\ m/s^2 < a < 1\ m/s^2$
180^o	1.2	*Uncomfortable*	$0.8\ m/s^2 < a < 1.6\ m/s^2$

DISCUSSIONS

Based on Figure 4,5, and 6, the vibrations on the vehicle body (sprung-mass) are effectively damped as a result of the vibrations on the vehicle's wheels (unsprung-mass). This is consistent with the VGS system prototype tests applied using the full-car method, where the results showed a 31% reduction in vertical acceleration on bumpy road input [13]. This demonstrates that the VGS system plays a crucial role in damping vibrations in vehicles, focusing on comfort and safety during driving [11].

Table 6 presents the RMS values of the sprung-mass to determine the comfort level of a vehicle. The table shows that the single-link angle of 90° has the lowest RMS value, 0.72 m/s², indicating a "fairly uncomfortable" rating according to ISO 2631. Meanwhile, the single-link angles of 0° and 180° indicate "uncomfortable" as their RMS values fall within the range of 0.8 m/s² to 1.6 m/s². The RMS results in this study are influenced by suspension stiffness (k_s) and suspension damping (c_s), while the damping of the unsprung-mass (c_t) and tire stiffness (k_t) were disregarded. As a result, the RMS values could not achieve optimal vibration damping in the vehicle. Additionally, the weight of the sprung-mass of the VGS prototype was neglected, preventing the system from maximizing comfort during operation. Therefore, the sprung-mass should be heavier than the unsprung-mass [11].

The average RMS value for the VGS system at a single-link angle of 90° ranged from 0.56 to 2.5 m/s² at speeds between 5 and 100 km/h [14]. This indicates that the experimental results are close to theoretical values. The average RMS value of the VGS system at a single-link angle of 90° was 0.546 m/s² at a constant speed of 20 km/h, using a full-car simulation in Matlab, which showed that the RMS value at a constant speed closely matches real-world test results [9]. Similarly, a full-car simulation of the VGS system found that actively controlling tire vibrations achieved a reduction with an RMS value of 5.17 m/s² [15]. The results of this study align with previous research, showing RMS values that are relatively consistent with existing findings.

CONCLUSION

The response of each single-link angle change on the VGS prototype to a bumpy road exhibits varying values. However, at all single-link angles, the system effectively dampens

the vibrations occurring as the wheel (unsprung-mass) passes over the bumpy road while maintaining the stability of the vehicle body (sprung-mass). Referring to the RMS values of the sprung-mass to determine vehicle comfort, the single-link angle of 90° has the lowest RMS value, 0.72 m/s², which indicates "Fairly uncomfortable" according to ISO 2631. Meanwhile, the highest RMS values are found at single-link angles of 180° and 0°, ranging between 0.8 m/s² and 1.6 m/s², categorized as "Uncomfortable" based on ISO 2631. The RMS results in this study are based solely on suspension stiffness (k_s) and suspension damping (c_s), while the damping of the unsprung-mass (c_t), tire stiffness (k_t), and the weight of the sprung-mass was disregarded.

REFERENCES

[1] F. T. K. Negara, I. Haryanto, and T. Prahasto, "Analisis Pengaruh Suspensi Terhadap Performa Pengereman Mobil Sedan Menggunakan Altair Motionview (in Indonesia)," *J. Tek. Mesin S-1*, vol. 12, no. 1, pp. 99–110, 2024.

[2] S. B. A. Kashem *et al.*, "A Study and Review on Vehicle Suspension System and Introduction of a HighBandwidth Configured Quarter Car Suspension System Functional, Sustainable, and Lightweight Materials View project Additive Manufacturing View project," *Aust. J. Basic Appl. Sci.*, no. July, pp. 59–66, 2015, [Online]. Available: https://www.researchgate.net/publication/342709347

[3] V. Gaikwad and A. S. Ugale, "Overview of Active Suspension System," *Int. Res. J. Eng. Technol.*, no. June, pp. 759–763, 2020, [Online]. Available: www.irjet.net

[4] A. R. Bhise, R. G. Desai, M. R. N. Yerrawar, A. C. Mitra, and D. R. R. Arakerimath, "Comparison Between Passive And Semi-Active Suspension System Using Matlab/Simulink," *IOSR J. Mech. Civ. Eng.*, vol. 13, no. 04, pp. 01–06, 2016, doi: 10.9790/1684-1304010106.

[5] A. An-Nizhami, N. Apriandi, P. Yanuar, and W. I. Nugroho, "Pemodelan Sistem Suspensi Pasif dan Semi Aktif Regeneratif dengan Model Half Car dan Eksitasi Harmonik (in Indonesia)," *J. Rekayasa Mesin*, vol. 17, no. 2, p. 297, 2022, doi: 10.32497/jrm.v17i2.3720.

[6] M. McCallig and V. Pakrashi, "Whole-Body Vibration Exposure from incubators in the Neonatal care Setting: A Review.," *J. Env. Occup Heal.*, vol. 11, no. 2, pp. 37–46, 2021.

[7] T. Yuvapriya, P. Lakshmi, and S. Rajendiran, "Vibration control and performance analysis of full car active suspension system using fractional order terminal sliding mode controller," *Arch. Control Sci.*, vol. 30, no. 2, pp. 295–324, 2020, doi: 10.24425/acs.2020.133501.

[8] C. Arana, S. A. Evangelou, and D. Dini, "Series active variable geometry suspension for road vehicles," *IEEE/ASME Trans. Mechatronics*, vol. 20, no. 1, pp. 361–372, 2015, doi: 10.1109/TMECH.2014.2324013.

[9] C. Arana, S. A. Evangelou, and D. Dini, "Series Active Variable Geometry Suspension application to comfort enhancement," *Control Eng. Pract.*, vol. 59, no. December 2016, pp. 111–126, 2017, doi: 10.1016/j.conengprac.2016.11.011.

[10] F. I. Abdi, U. Wasiwitono, H. Arizal, and A. H. Ramadani, "Kineto-Dynamic Pada Variable Geometry Suspension (VGS) (in Indonesia)," *J. Rekayasa Mesin*, vol. 06, pp. 57–62, 2021.

[11] M. Yu, C. Arana, S. A. Evangelou, and D. Dini, “Quarter-Car Experimental Study for Series Active Variable Geometry Suspension,” *IEEE Trans. Control Syst. Technol.*, vol. 27, no. 2, pp. 743–759, 2017, doi: 10.1109/TCST.2017.2772912.

[12] M. I. ALFIAN, “Analisis Pengaruh Perubahan Geometri Suspensi Terhadap Dinamika Getaran Honda Cbr 150R (in Indonesia),” Institut Teknologi Sepuluh Nopember (ITS), 2018.

[13] M. Yu, C. Cheng, S. A. Evangelou, and D. Dini, “Robust Control for a Full-Car Prototype of Series Active Variable Geometry Suspension,” *Proc. IEEE Conf. Decis. Control*, vol. 2019-Decem, no. Cdc, pp. 7615–7622, 2019, doi: 10.1109/CDC40024.2019.9029344.

[14] F. I. Abdi, *Analisis Dinamis pada Variable Geometry Suspenssion (VGS) dengan Kendali LQR dan LQG* (in Indonesia), no. 1. Surabaya, Indonesia: Institut Teknoligi Sepuluh November (ITS), 2018.

[15] M. Yu, C. Cheng, S. Evangelou, and D. Dini, “Series Active Variable Geometry Suspension: Full-Car Prototyping and Road Testing,” *IEEE/ASME Trans. Mechatronics*, vol. 27, no. 3, pp. 1332–1344, 2022, doi: 10.1109/TMECH.2021.3097153.